GEORGIA INSTITUTE OF TECHNOLOGY OFFICE OF CONTRACT ADMINISTRATION

PROJECT ADMINISTRATION DATA SHEET

[X] ORIGINAL

[ ] REVISION NO. ____

Project No. E-19 647 DATE: 4/4/81

Project Director: Dr. E. A. Starke, Jr. School/~~Dept~~ Chemical Engineering

Sponsor: Exxon Education Foundation; New York, New York 10020 ~~mac~~

Type Agreement: Grant Letter dated 2/13/81, w/check

Award Period: From 2/13/81 To Open (Performance) ----- (Reports)

Sponsor Amount: $5,000 Contracted through:

Cost Sharing: None ~~GTRI~~/GIT

Title: Support of Research Activities in the Fracture and Fatigue Lab

ADMINISTRATIVE DATA OCA CONTACT Duane Hutchison x 4820

1) Sponsor Technical Contact:

2) Sponsor Admin./Contractual Contact: Mr. Richard R. Johnson, Research Director; Exxon Education Foundation, 111 West 49th Street, New York, New York 10020 (212) 398-2273

Reports: See Deliverable Schedule Security Classification: None

Defense Priority Rating: None

RESTRICTIONS

See Attached N/A Supplemental Information Sheet for Additional Requirements.

Travel: Foreign travel must have prior approval - Contact OCA in each case. Domestic travel requires sponsor approval where total will exceed greater of $500 or 125% of approved proposal budget category.

Equipment: Title vests with GIT

COMMENTS:

COPIES TO:

Administrative Coordinator
Research Property Management
Accounting Office
Procurement Office
Research Security Services
~~Reports Coordinator~~ (OCA)
Legal Services (OCA)
Library, Technical Reports
EES Research Public Relations (2)
Project File (OCA)
Other:

GEORGIA INSTITUTE OF TECHNOLOGY OFFICE OF CONTRACT ADMINISTRATION

SPONSORED PROJECT TERMINATION/CLOSEOUT SHEET

Date April 3, 1984

Project No. E-19-647 School/~~Lab~~ ChE

Includes Subproject No.(s)

Project Director(s) Dr. E.A. Starke, Jr. ~~GTRI~~ / GIT

Sponsor Exxon Education Foundation; NY, NY

Title Support of Research Activities in the Fracture and Fatigue Lab

Effective Completion Date: 4/2/84 (Performance) (Reports)

Grant/Contract Closeout Actions Remaining:

- [x] None
- [ ] Final Invoice or Final Fiscal Report
- [ ] Closing Documents
- [ ] Final Report of Inventions
- [ ] Govt. Property Inventory & Related Certificate
- [ ] Classified Material Certificate
- [ ] Other

Continues Project No. Continued by Project No.

COPIES TO:

Project Director
Research Administrative Network
Research Property Management
Accounting
Procurement/EES Supply Services
Research Security Services
Reports Coordinator (OCA)
Legal Services

Library
GTRI
Research Communications (2)
Project File
Other

INTRODUCTION

The susceptibility of high-strength wrought aluminum alloys to environmentally induced subcritical crack growth under sustained static tensile stress, usually referred to as stress-corrosion cracking (SCC), has been recognized as a significant factor in the proper application of these materials. One of the earliest uses of high strength aluminum alloys was in the aircraft industry, due to the relatively high strength-to-density ratios exhibited by these alloys. The forerunners to the modern 7XXX-series alloys were very high strength precipitation hardened Al-Zn-Mg alloys developed in 1923 for application in the rigid airship, Zeppelin, but the first shipment of fabricated parts cracked during transport to the airship factory.[1] The failures were attributed to SCC under the combined influence of residual tensile stresses and humidity. The three most important factors associated with this and the majority of stress-corrosion failures are: 1) the introduction of a new alloy with higher yield and tensile strength than alloys previously used, 2) residual or assembly stresses in the alloy, and 3) exposure to the moisture of the air.

Intergranular crack propagation is dominant in the SCC of aluminum alloys as a result of stress-corrosion resistance being strongly related to the local grain shape and orientation with respect to the applied stress. Most stress-corrosion failures of aluminum alloys have resulted from residual or assembly surface tension stresses acting continuously in the short-transverse direction (or transverse in the case of round and square sections) relative to the grain structure.[2] The decrease in load-sustaining capability resulting from SCC is frequently related to a threshold stress, σ_{SCC}, which is the minimum stress at which SCC is observed within a given time. Mechanical, fracture, and stress-corrosion properties for several 7XXX-series aluminum alloys are given in Table I.[1]

Localized decomposition of solid solution at the grain boundaries is characteristic of the microstructure in tempers that are susceptible to SCC. In most cases, precipitation in the grain boundaries can be established, and any alloying addition or metallurgical treatment that affects the precipitation sequence or grain shape can influence the resistance of these alloys to SCC.[3] Stress corrosion resistant tempers have been developed for the Al-Zn-Mg-Cu system (such as 7075-T73), but other tempers (i.e., T6 type) remain susceptible to SCC especially in the short transverse direction. Less success has been achieved in developing stress-corrosion resistant tempers in the copper-free Al-Zn-Mg alloys, which display susceptibility to SCC in a wider range of environments.

THEORIES

Mears, Brown and Dix proposed a generalized theory of stress corrosion in metals.[3,4] Localized corrosive attack by the environment produces fissures, and concentration of normal components of tensile stress relative to the path of corrosive attack develops at the base of the fissures. The preferentially corroded paths may represent strata of relatively low inherent resistance to corrosion or they may be anodic relative to the surrounding metal. As a fissure grows in length and the radius of the base decreases, the magnitude of the stress concentration increases. Further opening (cracking) of the fissure will occur as a result of stress concentration at the base, exposing new metal to the corrosive environment. Corrosion of the freshly exposed metal surfaces is accelerated due to their anodic potential, and current flow from the crack tip will increase until protective films are reformed. Continued corrosion results in further fissure extension, and ultimately, the combined effects of tensile stress and corrosion result in crack growth. The paths of preferential corrosion are usually associated with grain boundaries in aluminum alloys.

Specific theories on the mechanisms of SCC are based upon a thorough understanding of the precipitation sequences in the 7XXX-series aluminum alloys, and the resulting effects upon the physical and chemical metallurgy of these alloys. Spherically shaped Guinier-Preston (GP) zones are generated during the aging of Al-Zn-Mg alloys at temperatures up to 260°F.[5] Aging times and temperatures characteristic of the T6 temper (highest strength) produce GP zones with an average diameter of 20 to 35 Å, along with very small amounts of a transition precipitate η', which is partially coherent on $(111)_{Al}$ planes. Strengthening effects have been attributed to the increased resistance to dislocation movement

resulting from stronger atomic bonds existing within the GP zones. When precipitates are coherent or partially coherent, the slip systems of the precipitates and the matrix are generally coincident, and the precipitates may be penetrated by dislocations. Aging at temperatures higher than those that produce maximum strength results in GP zone growth and greater amount of η'. This transition phase is considerably less effective in developing strength than the GP zone size. With higher temperatures or longer aging times, η' develops into a stable phase which can be $\eta(MgZn_2)$ or T $(Mg_3ZN_3Al_2)$ depending upon the composition of the alloy.

Copper additions to Al-Zn-Mg alloys of up to 1% do not change the basic precipitation mechanism.[3] Higher copper contents allow greater precipitation hardening, with some contribution of copper atoms to zone formation. The composition of the η phase in the Al-Zn-Mg-Cu system can vary, and it has not been established for Al-rich alloys. Along with the heterogeneous precipitation of phases at grain boundaries during thermal treatments of aluminum alloys, solute depleted regions may develop at the grain margins. These regions of the microstructure may be relatively free of precipitate phases, and exhibit different chemical and mechanical properties when compared with the grain bodies and boundaries.

Thomas and Nutting observed that intercrystalline mechanical fracture of 7XXX-series aluminum alloys near maximum hardness was related to preferential slip in the precipitate-free zones (PFZ) adjacent to the grain boundaries.[3,5] The absence of precipitates in the grain margins was attributed to vacancy migration to grain boundaries during quenching, resulting in a reduction of nucleation sites within the margin. Stress concentration effects in aluminum alloys usually develop at grain boundaries, and dislocation movement can occur in

the adjacent precipitate free zones under applied stresses less than the yield stress of the material. Strain in an alloy in the peak hardened condition will result in preferential plastic flow in the grain margins. If this strain is induced in a corrosive environment, preferential corrosive attack will develop along the regions where plastic flow has occurred. Therefore, intercrystalline SCC can occur under a sustained tensile stress in active environments.

Gruhl theorized that stress corrosion crack sensitivity of an Al-5Zn-3Mg-0.3Mn-0.15Cr was associated with zones which are related to single phase segregation in the matrix, rather than with the heterogeneous precipitates at grain boundaries.[3,6] Experiments performed upon this alloy by Gruhl and Cordier led to the theory that stress corrosion is caused by metastable redissolvable precipitates, and that precipitation of stable phases can lead improved resistance to SCC.

Jacobs hypothesized that the quench-induced dislocation structure observed in the T6 temper was vital to the initiation of stress corrosion cracks.[3,7] Pitting in both the T6 and T73 develops by the dissolution of large $MgZn_2$ precipitate particles in grain boundaries and grains, however, the stress corrosion behavior in these tempers is significantly different. Jacobs concluded that the critical role of dislocations was to assist in the nucleation of cracks of appropriate geometry for propagation. In later works, Jacobs suggested that the contribution of dislocations to stress corrosion susceptibility was more significant when they were strongly pinned, or immobile; and that an increase in precipitate-particle density lowered stress corrosion resistance more than increased dislocation density.

Holl rejected the views of both Thomas and Jacobs after performing electron microscopic examinations of the deformation behavior of an Al-5.7Zn-2.7Mg-0.5Cu

alloy in various states of susceptibility to SCC.[3,8] Holl concluded that the SCC behavior of this alloy is controlled by the mode of deformation, which is a function of the structural condition of the matrix. When this alloy is aged to contain GP zones or coherent precipitates, it will be highly susceptible to SCC. In this condition, slip is concentrated in well defined slip bands and dislocations show a marked tendency to remain on their original slip planes. The formation of non-coherent precipitates, usually through over-aging, results in the best resistance to SCC. In the highly resistant condition, restricted slip does not occur and dislocations form uniformly distributed tangles. Sprowls and Brown reported that, "Experience at the Alcoa Research Laboratories supports Holl's contention that neither the presence per se of a precipitate-free grain boundary region or a quench-induced dislocation structure governs the resistance to SCC of Al-Zn-Mg-Cu alloys."[3]

In attempting to establish microstructures characteristic of susceptibility (or resistance) to SCC, it is important to study the role of the electrochemical relationships of the different phases with the environment. Materials with microstructures identified as susceptible to SCC fail in some aqueous electrolytes and remain unaffected in other electrolytes. Hunter, Frank and Robinson studied corrosion of thin films of slowly quenched 7075-W alloy sheet using transmission electron microscopy techniques, and observed extremely selective corrosion which extended along grain margins leaving particles of grain boundary precipitate unattacked.[5] Fink and Willey observed that the partial depletion of copper, zinc and magnesium from the solid solution at the grain boundary regions of slowly quenched sheet causes the grain margins to become anodic to both the grain bodies and the $Mg(Al, Cu, Zn)_2$ phase precipitated in the grain boundaries.[3,9] Investigations of the effect of artificial aging on the electrochemical potential of rapidly quenched 7075-W sheet revealed that aging at 250°F resulted in a potential shift of about 75 mv in the cathodic direction after 24 to 36 hours and

no further change after 48 hours of total aging.[3] However, if this alloy is aged for 8 hours at 350°F after aging for 24 hours at 250°F, the potential shifts about 35 mv in the anodic direction.

The initial potential change with aging indicates the precipitation of zinc from solid solution at the lower temperature. The second aging step reduces copper and zinc in solid solution in the grain bodies, causing the grains and grain boundaries to approach the same potential. This type of electrochemical response to aging could account for the greater resistance of 7075-T73 short transverse specimens machined from thick sections compared to 7075-T6.[3] The electrochemical mechanism for intergranular susceptibility in Al-Zn-Mg-Cu alloys appears to be markedly influenced by the extent of copper removal from solid solution, rather than by a concentration of solute elements in the precipitate-free region. The determination of an electrochemical model for Al-Zn-Mg alloys is controversial, but the two models given most consideration involve anodic components of: 1) grain boundary precipitates such as $MgZn_2$, or 2) plastically strain precipitate free grain boundary regions.

A theory on the mechanism of SCC in Al-Zn-Mg alloys involving hydrogen was proposed by Haynie and Boyd.[10] This theory was based on the absorption of hydrogen into grain boundary regions. The mechanically weaker depleted zones, in precipitation hardening alloys can plastically deform at relatively low stresses. The small volume of the zones, however, restricts the total amount of plastic flow that can occur, and small notches may form at grain boundaries. The material at the notch root is in a triaxial state of stress and has a higher hydrostatic-stress component than the grain that is subjected only to a uniaxial tensile stress. Haynie and Boyd proposed that, "The hydrostatic-stress component causes preferential absorption of hydrogen, which in turn causes an increase in the activation energy

for dissolution of the grain boundary material".[10]

The possibility that an oxide film is always present on the corroding surface and that the kinetics may be controlled by the rate of diffusion of cations through the oxide was considered by Haynie and Boyd.[10] Since mechanical rupture of the oxide film is less likely when the material is stressed below its bulk-flow stress, the film rupture mechanism does not entirely account for observed SCC behavior at this lower stress level. Electrochemical studies by Haynie and Boyd lead to speculation on other possible influences of hydrogen on SCC, which were: 1) hydrogen absorbed into grain boundaries may accelerate localized attack by increasing the cation gradient through the strained oxide film, allowing accelerated diffusion of aluminum ions and 2) the relative distribution of protons in the oxide at grains and grain boundaries may cause preferential grain boundary attack.

FRACTURE MECHANICS

The treatment of the stress aspect of SCC through a linear-elastic fracture mechanics involves the stress-intensity factor, K. If a uniform tensile stress is applied to a plate of metal in the presence of a short crack, the elastic stress field at the leading edge of the crack can be characterized by the single parameter, K, which is proportional to the product of the nominal stress and the square root of the crack size.[11] The parameter K is a quantitative measure of the intensification of the stress at the crack tip. The magnitude of K increases with increasing stress or increasing crack size. Unstable fast fracture occurs when this parameter reaches a sufficiently high value, K_c, which is often called the fracture toughness. Values for K_c vary with specimen thickness, but at a certain thickness, the fracture toughness reaches a lower limiting value.

Specimens of this thickness (or thicker) are described as being in the state of plane strain when fracturing, and the limiting value of fracture toughness is described as the plane-strain fracture toughness, K_{Ic}. The subscript I indicates that the crack grows in the opening mode.

Aluminum alloys of practical importance have sufficient ductility such that a stress across a crack produces a plastic zone ahead of the crack. The plastic zone formation produces a crack opening displacement (COD), which has been estimated for plane-stress conditions in terms of K, Young's modulus E, and yield strength σ_y by the following equation:[11]

$$\text{opening crack displacement} = \frac{K^2}{E\sigma_y}$$

Multiplication of the right-hand term by the reciprocal of the triaxial stress-intensification factor gives the displacement for plane strain conditions. In the absence of corrosion, this equation indicates a finite opening of a crack normal to the crack plane.

Propagation of stress-corrosion cracks through plane-stress plastic zones is extremely slow, or may not occur.[11] As a given material is tested in progressively thinner specimens, the plane-stress plasticity effects become progressively more important, until stress-corrosion cracking does not occur (for all practical purposes). Stress-corrosion crack growth under constant loading conditions is accompanied by increases in the stress intensity, and the plane-stress plastic zone increases in the x and z directions according to the equation shown in Figure 1.[12] The reluctance of stress-corrosion cracks to propagate through the plane-stress plastic zone at the sample surface makes the direct observation of stress-corrosion crack-growth kinetics difficult.

In quantification of the stress intensity responsible for SCC, the thickness of the specimen should be sufficient for the effects of the plane-stress zone to be negligible. This thickness depends on the stress intensity used and the yield strength of the material. The most conservative recommendation is that the thickness should be at least $2.5\ (K/\sigma_y)^2$.[11,12]

One of the main purposes of fracture mechanics is to have a means for predicting the behavior of a given metal or alloy in service from small sample observations. A typical surface-cracked specimen is shown in Figure 2[11] along with the equation for K. This relationship provides a correlation between K_{ISCC} and the various combinations of stress (σ) or load (P), flaw depth (σ_o), and flaw shape (ϕ). For determining the depth of a long surface crack that would be sufficient for stress-corrosion crack propagation at yield-point stress levels, this equation reduces to:

$$a_{cr} = 0.2\left(\frac{K_{ISCC}}{\sigma_y}\right)^2$$

where a_{cr} is the critical crack depth expected to propagate SCC. In design, this could be used to estimate the maximum tolerable flaw size for a loading situation adequately represented by the surface-cracked specimen configuration and deformation mode. Numerical solutions of K_I for other practical test specimens have been established.[11,12]

The basis and limitations for using the crack-tip stress-intensity factor, K_I, to characterize the crack-driving force in subcritical-crack growth have been considered by Wei.[13] The opening mode, I, was discussed, but the considerations were applicable to the edge-sliding mode, II, and the tearing mode, III. The stress and displacement fields associated with the opening mode in an isotropic elastic body are:

$$\sigma_x = \frac{K_I}{\sqrt{2\pi r}} \cos\frac{\theta}{2}\left[1 - \sin\frac{\theta}{2}\sin\frac{3\theta}{2}\right]$$

$$\sigma_y = \frac{K_I}{\sqrt{2\pi r}} \cos\frac{\theta}{2}\left[1 + \sin\frac{\theta}{2}\sin\frac{3\theta}{2}\right]$$

$$\sigma_{xy} = \frac{K_I}{\sqrt{2\pi r}} \sin\frac{\theta}{2}\cos\frac{\theta}{2}\cos\frac{3\theta}{2}$$

$$u = \frac{K_I}{8\mu}\sqrt{\frac{2r}{\pi}}\left[(2\kappa - 1)\cos\frac{\theta}{2} - \cos\frac{3\theta}{2}\right]$$

$$v = \frac{K_I}{8\mu}\sqrt{\frac{2r}{\pi}}\left[(2\kappa + 1)\sin\frac{\theta}{2} - \sin\frac{3\theta}{2}\right]$$

For plane strain:

$$\kappa = 3 - 4\nu$$
$$\sigma_z = \nu(\sigma_x + \sigma_y)$$
$$w = 0$$

For generalized plane stress:

$$\kappa = \frac{3 - \nu}{1 + \nu}$$

$$\sigma_z = 0$$

$$w = -\frac{\nu}{E}\int(\sigma_x + \sigma_y)\,dz$$

where r and Θ are the radial and angular coordinates measured from the crack tip (Figure 3); μ is the shear modulus, and ν is the Poisson's ratio. These stresses and displacements are considered to be good approximations in the region where r is small compared to other planar dimensions. K_I is the stress intensity factor for mode I, as previously discussed.

Although the linear elasticity solution for a sharp crack results in infinite stresses at the crack tip where the radius of curvature is "zero," the deformed shape of the crack assumes some finite radius of curvature and the stress level remains finite.[13] Reduction of the stress concentrating effects of the crack also occurs due to the local plastic deformation at the crack tip. The stress distribution as a whole will not be seriously disturbed if the zone of plastic deformation is small relative to the crack length and other planar dimensions of the body. Under these conditions, the elasticity solutions represent a reasonably accurate approximation of the stress and displacement fields near the crack tip. Containment of the small plastic zone at the crack tip by surrounding elastic material results in a general behavior of the region governed by this surrounding elastic material, and therefore characterization by the crack-tip stress-intensity factor, K_I, is reasonable. The use of this parameter to characterize the crack driving force is "predicated on the assumption of limited plasticity."[13]

Wachtman presented a survey of the, "current knowledge of those aspects of fracture in brittle ceramics and glasses which can be understood in a unified way in terms of the quantitative science of crack behavior."[14] In this paper, slow crack propagation by stress corrosion was presented in fracture mechanics terms. Griffith theory predicts that cracks do not propagate below the critical stress required for rapid propagation to failure. However, slow propagation of cracks in glass is well established, and Charles and Hillig assumed that the rate of crack propagation in glass is controlled by a chemical reaction between the glass and the water in the environment.[14,15]

It was theorized that the crack velocity should be dependent on an activation energy which in turn should depend on stress. The relationship expressing

the velocity of chemically assisted crack growth proposed by Charles and Hillig was:[14,15]

$$V = Vo \exp(-E^{\neq} + V^{\neq} \sigma_t - V_M\gamma/\rho)/RT$$

where $E^{\neq}$ is the stress-free activation energy, $V^{\neq}$ the activation volume, σ_t the stress at the crack tip, V_M the molar volume of the glass, γ the interfacial surface energy between glass and the reaction products, and ρ the radius of the crack tip. Weiderhorn and Bolz expressed this result in terms of K_I for a two-dimensional crack by using $K_I = \sigma(\pi\rho)^{\frac{1}{2}}/2$ to obtain:

$$V = Vo \exp[-E^* + 2V^{\neq} K_I/(\pi\rho)^{\frac{1}{2}}]/RT$$

where $E^* = E^{\neq} + V_M\gamma/\rho$.[14,16] This theory successfully describes many observations on environmentally dependent crack growth.

TESTING METHODS

Specimens for testing resistance to stress-corrosion can be grouped into three main types, which are smooth specimens or precracked specimens for external loading, and residual stress specimens.[17] Externally loaded smooth specimens include direct tension type, bent beams, u-bends, c-rings, o-rings and tuning forks. Generally, stressing by tensile loading constitutes a more severe test than the application of bending stress. Before fracture mechanics was developed and applied to the design of quantitative stress-corrosion tests, the conventional and more qualitative time-to-failure (TTF) test was employed to rate a materials susceptibility to SCC.[1] The TTF test involved exposure of a smooth, stressed specimen to a corrosive environment; ultimately determining a relationship between time-to-failure and the applied gross section stress. Due to the qualitative nature of the data resulting from TTF testing of smooth

samples (among other limitations), the testing of precracked specimens has become more developed and accepted recently.

Testing of precracked specimens by external loading makes use of linear elastic fracture mechanics to describe the stress distribution in a specimen containing a crack in terms of the stress intensity factor. The procedure involves mechanically precracking a specimen configuration for which the stress distribution is understood, and then loading the specimen to a predetermined stress intensity during exposure to an environment of interest. This test method, offers the following advantages over TTF testing of smooth samples, "1) the ability to state SCC thresholds in a form which can readily be analyzed in terms of resistance to catastrophic crack growth, 2) the ability to measure the rate of growth of stress-corrosion cracks..., and 3) the ability in the case of some alloy systems to avoid variable and prolonged periods of incubation of stress corrosion cracks."[17]

One of the most convenient specimen configurations and loading modes for studying stress-corrosion characteristics in aluminum alloys is the double-cantilever-beam (DCB) loaded by constant displacement to a stress intensity at or just below the critical stress intensity, K_{Ic}.[18] In this method, SCC will initiate rapidly (in susceptible materials) and proceed for a time at a fairly constant rate before slowing down as the crack lengthens and K_I decreases. If the crack growth stops, the stress intensity can be termed the threshold for SCC (K_{ISCC}). The data is usually plotted as crack propagation rate da/dt or V vs. stress intensity (K_I) A typical SCC crack-growth curve is shown in Figure 4 for a susceptible material (7079-T651).[18] The plateau velocity may be considered the highest SCC propagation rate that a material will sustain for significant crack extension. In this type of testing, the formation of corrosion

products within the crack can be continuous, and it may contribute to the stresses at the crack tip.

A joint Aluminum Association-American Society for Testing and Materials task group (ASTM G-1.06.91) has recommended a standard method of test for susceptibility to SCC of 7XXX aluminum alloy products (ASTM G 47-76). The proposed standard specifies corrosive environment and period of exposure, type of test specimen and method of loading, procedures for sampling various manufactured product forms, and guidelines for interpreting test results.[19] The standard is based on extensive round robin tests performed in nine different laboratories and long term atmospheric exposures. The data showed that a high degree of variability can be obtained in stress-corrosion test results for a given material depending on the test procedure.

The selection of the most appropriate test conditions depends on the metallurgy of the alloy, the mechanical properties of the product, and the chemistry of the test medium. Since stress is intimately involved in SCC, susceptibility to SCC can only be established by exposing both stressed and unstressed specimens to the environment of interest.

DISCUSSION

A number of theories and mechanisms for SCC in aluminum alloys have been developed, but because of the complexity of stress-induced environmental cracking in 7XXX-series alloys, critical data needed to establish the "true" mechanism of SCC remains undetermined. More than one correct theory may ultimately be established. Electrochemical effects, the nature of surface oxide films, and the heterogeneous metallurgical structure of these alloys must all be considered. The interactions of these factors under the influence of stress vary somewhat between the Al-Zn-Mg-Cu alloys and the copper free alloys in the 7XXX-series,

and at this time, greater success in developing SCC resistant tempers in the copper containing alloys has been achieved.

Holl's theory that SCC behavior of Al-Zn-Mg-Cu alloys is controlled by the deformation mode (and therefore the structural condition of the matrix) is supported by the results of research at Alcoa. Certainly the concentration of slip along PSB's has been established. A path of preferential corrosive attack may develop due to anodic potential in these plastically strained regions. Considerable data is available, however, that indicates the establishment of anodic regions due to solute segregation from the matrix in the form of precipitate phases. If grain margins were anodic to their surroundings as a result of solute depletion during heterogeneous precipitation at grain boundaries, selective intergranular corrosive attack would be enhanced without the influence of stress. Similarly, grain boundary precipitates with anodic potential could lead to intergranular attack. Protective oxide films develop rapidly in aluminum alloys, and the role of stress in disrupting these films certainly is an important factor in extending the selective attack of the environment. Significant changes in stress-corrosion crack velocity due to changes in the electrochemical activity of M precipitate phases as a function of copper content have been demonstrated.[20] One of the main advantages of copper additions in these alloys is copper's ability to dissolve in the matrix and enter the M phase, while increasing the nobility of both.

The application of fracture mechanics to the phenomenon of SCC is still in a developmental stage. Some success has been achieved in predicting stress corrosion behavior through fracture mechanics when compared with experimental data. The relationship developed by Hillig and Charles for ceramic application is particularly useful because of the additional chemical activity and molar

volume terms. Application of this relationship to metallic materials seems reasonable.

In general, the best approach to improving stress corrosion resistance in 7XXX-series alloys is through heat treatments. Redistribution of solute elements to decrease electrode potential differences of microconstituents and regions is one of the main goals. Some success has been achieved through alloying additions such as chromium. Overaging to produce incoherent precipitates while sacrificing some strength is effective in improving resistance.

Table 1 **Mechanical, Fracture, and Stress-Corrosion Properties for Several Aluminum Alloys**

Alloy temper	Thickness (in.)	Axis[1] of test spec	Minimum tensile strength		Min elong (% in 2 in or 4D)	Range in plane strain fracture toughness K_{Ic}			Basewise Stress corrosion threshold stress		
			Ultimate (ksi)	0.2% yield (ksi)		Long (ksi$\sqrt{in.}$)	Long trans (ksi$\sqrt{in.}$)	Short trans (ksi$\sqrt{in.}$)	Long (ksi)	Long trans (ksi)	Short trans (ksi)
Plates											
2014 T451	0.500-1.000	LT	58	36	14	≈40	≈38	17-25	--	--	--
2014 T651	0.500-1.000	LT	67	59	6	21-28	19-27	16-19	46	30	8
X7020 T651	1.275	LT	75	70	1.5	18-23	15-21	-	>57	>50	34
2021 T81	0.500-1.000	LT	≈87	≈58	3	26-37	21-34	--	>48	>48	35
2024 T351	0.500-1.000	LT	63	42	8	≈45	≈40	20-28	35	20	<8
2024 T62	0.500-3.000	LT	63	50	5	27	26	--	>50	>50	43
2024 T851	0.500-1.000	LT	68	58	5	20-32	20-32	16-24	>50	>50	40
2024 T86	0.500	LT	70	64	4	22	21	--	--	--	--
2124 T851[1]	1.001-1.449	LT	66	57	5	28	24	23	>50	>50	30
2219 T351	0.250-2.000	LT	46	28	10	>40	>40	--	--	--	--
2219 T37	0.040-2.000	LT	49	37	8	≈40	≈34	33	--	--	<10
2219 T62	0.250-1.000	LT	54	36	8	50	36	--	>34	--	>32
2219 T87	0.250-1.000	LT	64	51	7	26-29	24-28	20-30	>44	--	>41
RR 58	0.250	LT	≈58	≈45	≈8	27-34	28	--	>44	--	>40
5083 H112	0.250-1.500	L	40	18	12	≈40	≈38	--	--	--	--
5083 H321	0.188-1.500	L	44	31	12	≈45	≈45	--	>25	--	>25
5456 H112	0.250-1.500	L	42	19	12	≈38	≈38	--	--	--	--
5456 H321	0.625-1.250	L	46	33	12	≈45	≈45	30-33	--	--	--
8061 T651	0.500-1.000	LT	42	35	9	≈60	≈60	32-35	>38	--	>38
7001 T75	1.275	LT	77	66	4	19-26	17-23	--	>50	--	25
7005 T6351	0.250-3.000	LT	47	38	7	≈60	--	-	≈20	≈20	<20
X7007 T6		--	--	--	--	44	37	--	--	--	--
7019 T6151	0.250-2.000	LT	55	45	10	48	40	25-35	--	--	<5
7019 T63						44-45	36-37	20-25	>42	35	<8
7019 T64	up to 1.500	LT	80	61	9	>40	≈40	30-34	--	--	<5
X7050 T7351	--	--	-	--	--	38	30	28	--	--	--
7075 T651	0.500-1.000	LT	78	68	7	25-33	19-31	15-20	80	45	<8
7075 T7651	0.500-1.000	LT	71	60	8	31	23-26	22	>49	>49	26
7075 T7351	0.250-1.000	LT	69	57	7	30-41	24-36	19-21	>50	>48	>43
X7475 T7351	2.0	LT	≈59	≈49	--	52		36	>50	>48	>43
7079 T651	0.250-1.000	LT	74	65	8	25-34	22-28	15-18	>56	40	<8
7178 T651	0.500-1.000	LT	84	73	6	21-27	18-23	14-21	55	30	<8
7178 T7651	0.500-1.000	LT	73	62	8	26-30	21-28	17-19	>52	>52	25

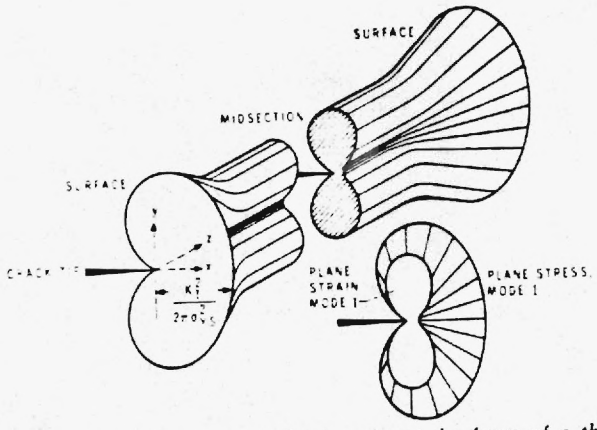

Fig. 1 —*Formal representation of plastic zone at the front of a through-thickness crack in a plate.*

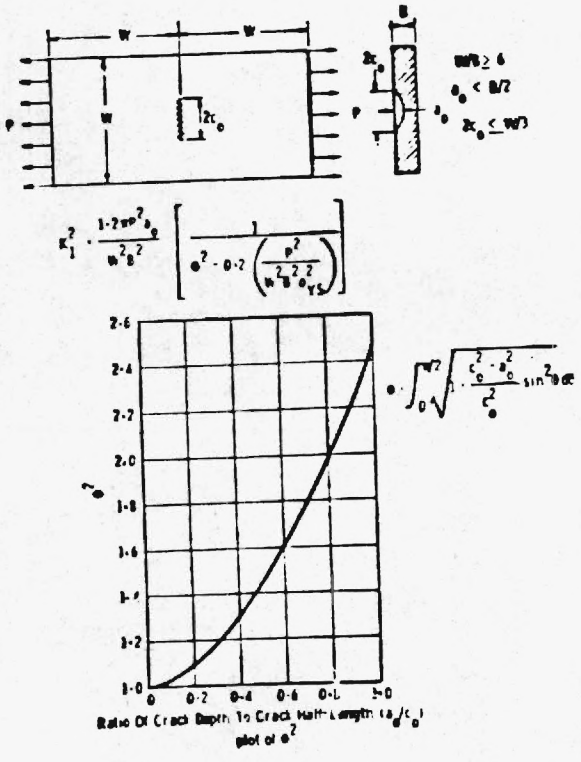

Fig. 2 Typical surface cracked specimen

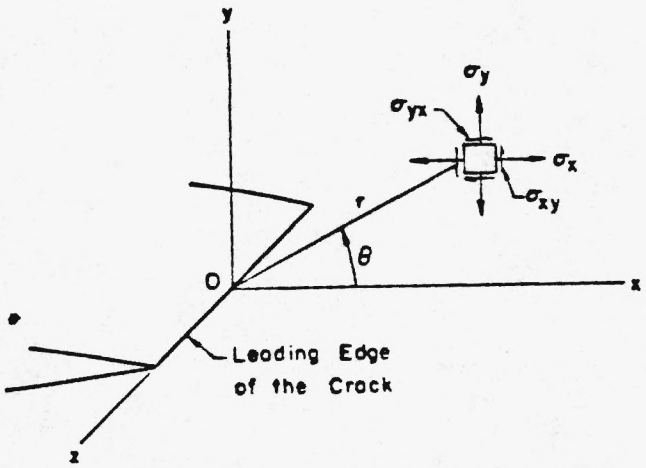

Fig. 3 – Coordinates and stress components in the crack-tip stress field.

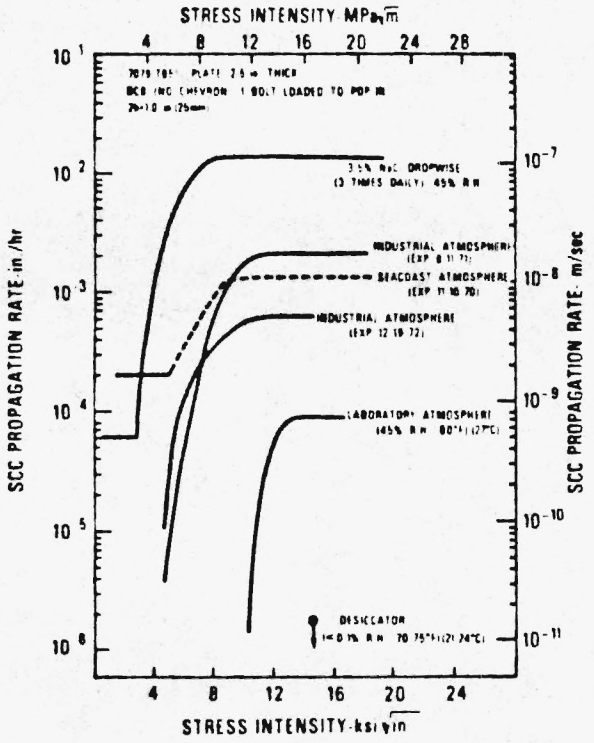

Fig. 4 —*Effect of corrosive environment on SCC propagation rate in 7079-T651 alloy plate (2.5 in. (64 mm) thick).*

REFERENCES

1. Markus O. Speidel and Michael V. Hyatt, "Stress-Corrosion Cracking of High-Strength Aluminum Alloys," Advances in Corrosion Science and Technology, Edited by M. G. Fontana and R. W. Staehle, vol. 2, p. 115-335, 1972.

2. D. O. Sprowls and R. H. Brown, "Resistance of Wrought High-Strength Aluminum Alloys to Stress Corrosion," Alcoa Technical Paper No. 17, p. 1-32, 1962.

3. D. O. Sprowls and R. H. Brown, "Stress Corrosion Mechanisms for Aluminum Alloys," in Proceedings of the International Conference on the Fundamental Aspects of Stress Corrosion Cracking, p. 466-506, NACE, Houston, TX, 1969.

4. R. B. Mears, R. H. Brown and E. H. Dix, Jr., "A Generalized Theory of Stress Corrosion of Alloys," Symposium on Stress Corrosion Cracking of Metals, published jointly by ASTM and AIME, p. 329, 1944.

5. G. Thomas and J. Nutting, "The Aging Characteristics of Aluminum Alloys-Electron Microscopic Studies of Alloys Based on the Aluminum-Zinc-Magnesium System," J. Inst. of Metals, vol. 88, p. 81, 1959-60.

6. Wolfgang Gruhl, "Electron Fractographic Studies on Stress Corrosion Cracking Samples of $AlZnMg_3$," Aluminium, vol. 38, p. 775, 1962.

7. A. J. Jacobs, "The Role of Dislocations in the Stress Corrosion Cracking of 7075 Aluminum Alloy," Trans. ASM, vol. 58, p. 579, April, 1965.

8. H. A. Holl, "Deformation Substructure and Susceptibility to Intergranular Stress Corrosion Cracking in an Aluminum Alloy," Corrosion, vol. 23, p. 173, June, 1967.

9. W. L. Fink and L. A. Willey, "Quenching of 75S Aluminum Alloy," Metals Technology, American Institute of Mining and Metallurgical Engineers, vol. 14, p. 5, August, 1947.

10. F. H. Haynie and W. K. Boyd, "An Electrochemical Study of the Mechanism of Stress Corrosion Cracking in an Aluminum-Zinc-Magnesium Alloy," in Proceedings of the International Conference on the Fundamental Aspects of Stress Corrosion Cracking, p. 580-589, NACE, Houston, TX, 1969.

11. B. F. Brown, "The Application of Fracture Mechanics to Stress-Corrosion Cracking," Metallurgical Reviews, No. 129, p. 171-183, 1968.

12. W. F. Brown, Jr. and J. E. Strawley, "Plane Strain Crack Toughness Testing of High Strength Metallic Materials," ASTM STP 410, American Society for Testing and Materials, p. 5, 1966.

13. R. P. Wei, "Application of Fracture Mechanics to Stress Corrosion Cracking Studies," in Proceedings of the International Conference on the Fundamental Aspects of Stress Corrosion Cracking, p. 104-112, NACE, Houston, TX, 1969.

14. John B. Wachtman, Jr., "Highlights of Progress in the Science of Fracture of Ceramics and Glass, " J. of Am. Cer. Soc., vol. 57, p. 509-519, December, 1974.

15. W. S. Hillig and R. J. Charles, High Strength Materials, Edited by V. F. Zackay, John Wiley & Sons, Inc., New York, p. 682-705, 1965.

16. S. M. Wiederhorn and L. H. Bolz, "Stress Corrosion and Static Fatigue of Glass," J. of Am. Cer. Soc., vol. 53, p. 543-548, October, 1970.

17. H. L. Craig, Jr., D. O. Sprowls, and D. E. Piper, "Stress-Corrosion Cracking," in Handbook on Corrosion Testing and Evaluation, Edited by W. H. Ailor, p. 231-290, 1971.

18. D. O. Sprowls, J. W. Coursen, and J. D. Walsh, "Evaluating Stress-Corrosion Crack-Propagation Rates in High-Strength Aluminum Alloys with Bolt Loaded Precracked Double-Cantilever-Beam Sepcimens," in Stress Corrosion-New Approaches, ASTM STP 610, American Society for Testing and Materials, p. 143-156, 1976.

19. D. O. Sprowls, T. J. Summerson, G. M. Ugiansky, S. G. Epstein, and H. L. Craig, Jr., "Evaluation of a Proposed Standard Method of Testing for Susceptibility to Stress-Corrosion Cracking of High-Strength 7XXX Series Aluminum Alloy Products," in Stress Corrosion-New Approaches, ASTM STP 610, American Society for Testing and Materials, p. 3-31, 1976.

20. B. Sarkar, M. Marek, and E. A. Starke, Jr., "The Effect of Copper Content and Heat Treatment on the Stress Corrosion Characteristics of Al-6Zn-2Mg-XCu Alloys," Met. Trans. A, vol. 12A, p. 1939-1943, November, 1981.